Provided for non-commercial research and educational use only.
Not for reproduction or distribution or commercial use.

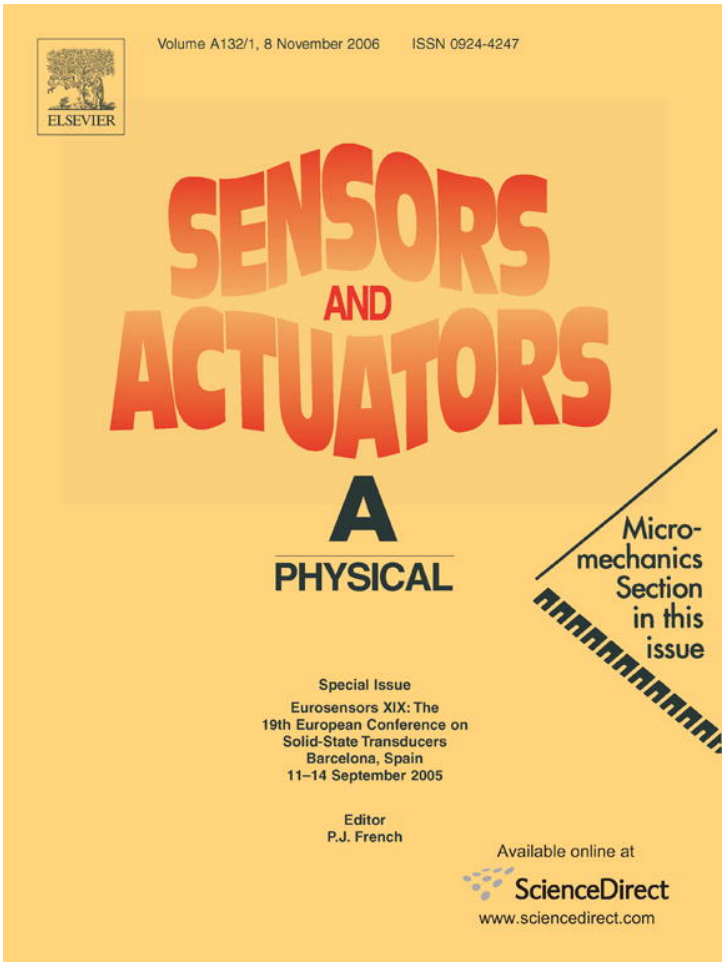

This article was originally published in a journal published by Elsevier, and the attached copy is provided by Elsevier for the author's benefit and for the benefit of the author's institution, for non-commercial research and educational use including without limitation use in instruction at your institution, sending it to specific colleagues that you know, and providing a copy to your institution's administrator.

All other uses, reproduction and distribution, including without limitation commercial reprints, selling or licensing copies or access, or posting on open internet sites, your personal or institution's website or repository, are prohibited. For exceptions, permission may be sought for such use through Elsevier's permissions site at:

http://www.elsevier.com/locate/permissionusematerial

Available online at www.sciencedirect.com
ScienceDirect
Sensors and Actuators A 132 (2006) 56–62
SENSORS AND ACTUATORS A PHYSICAL
www.elsevier.com/locate/sna

New cost-effective sensor for the characterization of automotive headlamps by measurements in the near field

S. Royo [a,*], M.J. Arranz [a], J. Arasa [a], M. Cattoen [b], T. Bosch [b]

[a] *Center for Sensor, Instrumentation and Systems Development, Technical University of Catalunya (UPC-CD6), Rambla Sant Nebridi 10, E08222 Terrassa, Spain*

[b] *Laboratoire d'Electronique de l'ENSEEIHT, Institut National Polytechnique de Toulouse (INPT-LEN7), Rue Charles Camichel 2 BP7122, 31071 Toulouse, France*

Received 23 September 2005; received in revised form 24 April 2006; accepted 27 May 2006
Available online 7 July 2006

Abstract

Nowadays, European Normative regarding headlamp validation evaluates the photometric distribution of the source as a series of illumination values measured at a plane placed 25 m away from the light source. An innovative and inexpensive approach to test this photometric distribution is presented. We propose to sample the luminance field at a plane placed a few centimetres in front of the headlamp displacing a CCD camera at an adjustable number of positions. A specific processing of the sequence images allows simultaneously measuring the direction of propagation through deflectometric techniques and the energy of the light beams leaving the source through photometric techniques. Image-processing techniques may then be applied to these data in order to evaluate the photometric distribution in any predefined distant surface. An overview of the unit, of the measurement principle, and of the main calibrations performed is presented along the paper. In particular, the techniques for the calibration of the global constant converting CCD grey level values into photometric units are described and applied to different distributions. Finally, the comparison of computed illumination maps using the unit with reference measurements at photometric tunnels is presented, showing good agreement and demonstrating the validity of the approach.
© 2006 Elsevier B.V. All rights reserved.

Keywords: Automotive; Headlamps; Photometry; Near-field; Optical testing; CCD; Light sources

1. Introduction

Transport by road has been proved to be the most dangerous of all transport modes [1]. In the European Union, European Transport Policy is pursuing objectives as ambitious as to halve the number of accidents by 2010 through improving road safety by using new technologies. In addition, night-time is the most dangerous moment of the day for drivers. It has been shown that, although the traffic at night is only 25% of the traffic at daytime, there is a similar amount of traffic fatalities in both periods [2]. Although a great number of factors are involved in these accidents, such as fatigue or alcohol, the reduction of the visibility of the road is clearly a key aspect of the problem [3]. So, enhancing automotive lighting designs should play a key role in the goal of improving the safety of drivers in night-driving conditions. In this sector, new technologies and source types are being incorporated year after year according to design and fashion trends, while at the same time the headlamp should still provide the best possible illumination of the road in front of the vehicle and avoid glare effect for the rest of the drivers.

Nowadays, headlamp designs are validated in photometric tunnels according to European Normative. In such installations, the illumination distribution is measured in a plane placed 25 m away from the headlamp through a mechanical goniophotometer [4,5], a bulky mechanical device which allows orienting the headlamp with high accuracy towards a distant, point-shaped high accuracy photometer. This approach has the main drawbacks of the mechanical complexity of the measuring system, plus the large space requirements. This has pushed some alternative methods to simplify the measurement to be proposed. One of the most relevant is the multiphotometer, which becomes more compact by introducing a large lens which projects the image distribution in a screen once the headlamp has been placed at its focus. The screen has a number of photometers on it mea-

* Corresponding author. Tel.: +34 93 7398904; fax: +34 93 7398923.
E-mail address: royo@oo.upc.edu (S. Royo).

0924-4247/$ – see front matter © 2006 Elsevier B.V. All rights reserved.
doi:10.1016/j.sna.2006.05.032

Author's personal copy

suring the final distribution. However, the alignment and the positioning of the headlamp in this system are critical, yielding the whole approach impractical. Recently, the same principle has been proposed using a radiometric CCD camera instead of the multi-detector screen.

In our approach, a combination of deflectometric, photometric and image processing techniques allows to calculate the distribution in any distant surface from a discrete number of measurements performed in a plane close to the headlamp. Hence, the sensor will compute the illumination distribution in the far field from measurements in the near field. In addition, our approach is much more cost-effective than currently used techniques. Although the system has been developed to characterize headlamp distributions, it has been successfully applied to other types of light sources, such as automotive pilots, halogen lamps or even LEDs.

The paper has been divided into five sections. After this introduction we will present the basics of the measurement principle of the unit. Next, the experimental prototype built to demonstrate the validity of the approach is presented. Subsequently, the photometric calibration of the system is explained and the calculated illumination distributions in photometric units will be compared to measurements performed in a reference photometric tunnel. The last section exposes the main conclusions of the work and points out possible applications.

2. Measurement principle

The main sensor in the unit is a commercial CCD camera which is displaced across the measurement plane through a computer-driven two-dimensional motor unit. The CCD camera performs a double sensing task. On one side, it measures the direction of the travelling energy through the position of the pixels where the incoming energy is impinging. On the other side, it measures the energy propagating along each direction through the grey level value of the corresponding pixel. The direction of the travelling energy may be measured from the pixel position by keeping the lens of the CCD camera focused at infinity. This particular lens configuration makes all rays with a given slope to impinge on the same pixel [6], so that they may be identified with a single light ray (Fig. 1). The two-dimensional slope (u, v) of each of the rays may then easily be calculated following:

$$u = \frac{n_x \Delta x}{f'}, \qquad v = \frac{n_y \Delta y}{f'} \tag{1}$$

where f' is the focal length of the lens, n_x (n_y) the number of pixels from the centre of the array along $X(Y)$ axis, Δx (Δy) is the size of the pixel of the CCD along $X(Y)$ axis, and $u(v)$ is the slope of the wavefront along $X(Y)$ axis. The energetic flux value (F) associated to each direction of propagation is then determined using the grey level of the considered pixel. This means for each pixel of a register we collect information on a ray passing through the center of the lens (x, y) with slope (u, v) and energy F.

To completely characterize the illumination distribution in a plane close to the headlamp, the sensor is displaced across the measurement plane in a regularly spaced array of measurement points, registering both the direction of propagation of the energy (u, v) and its amount F at each of the measurement points (x, y). As the total energy recorded in each register depends on the aperture of the lens, a correction factor to compensate for the different areas covered by the aperture (round) and the displacement (square) of the lens is required to properly compute the final illumination distribution.

Once the sensor has acquired a sequence of registers from the luminance field of the headlamp in the near field, the final distribution in the far field is computed. Due to the amount of information collected by the sensor, the classical ray-tracing approach causes very high computational effort. Therefore, a simpler algorithm was preferred based on the projection and accumulation of shifted registers in the final plane. With this approach, the computing time of the far-field distribution is reduced to a couple of seconds. A final calibration step for converting these accumulated grey level values into photometric units is then required, and will be presented in an independent section.

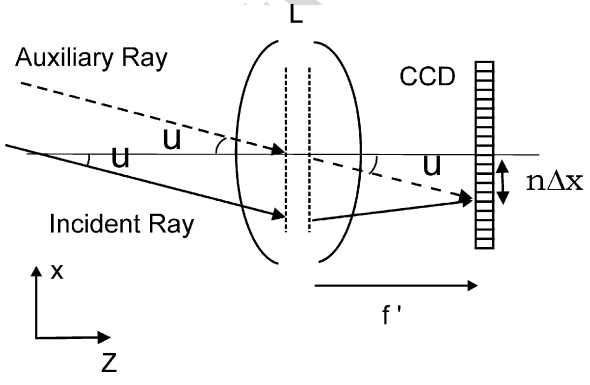

Fig. 1. Measurement of slope (u) with a lens focused to infinity using a CCD sensor.

3. Set up

A robust prototype of the measurement apparatus capable for operation in industrial environments has been constructed, tested and calibrated. The headlamp is placed in a fixed position in front of the sensor. As shown in Fig. 2, a two-dimensional motorized mechanical setup permits the displacement of the sensor along X and Y axes with a positioning repeatability of 10 μm.

The sensor comprises a commercial CCD camera, a lens, a photopic filter, and neutral filters. Furthermore, a frame grabber and a computer are required to record and store the registers in all the positions in the measurement plane. A 1.7:17 lens was selected, with a 17.2 mm focal length and a distortion value below 0.5% in all the CCD area. The illumination fall-off at edge of field due to vignetting was selected to be as small as possible, keeping transmittance over 90% in all the field of view. An equalizing filter and a standard photopic filter achieved a spectral response for each pixel equivalent to that of a standard photometer. Calibrated neutral filters with flat spectral response were used to adjust the sensitivity of the sensor to the energy output of the headlamp. The oscillations in transmittance in the

horia personal copy

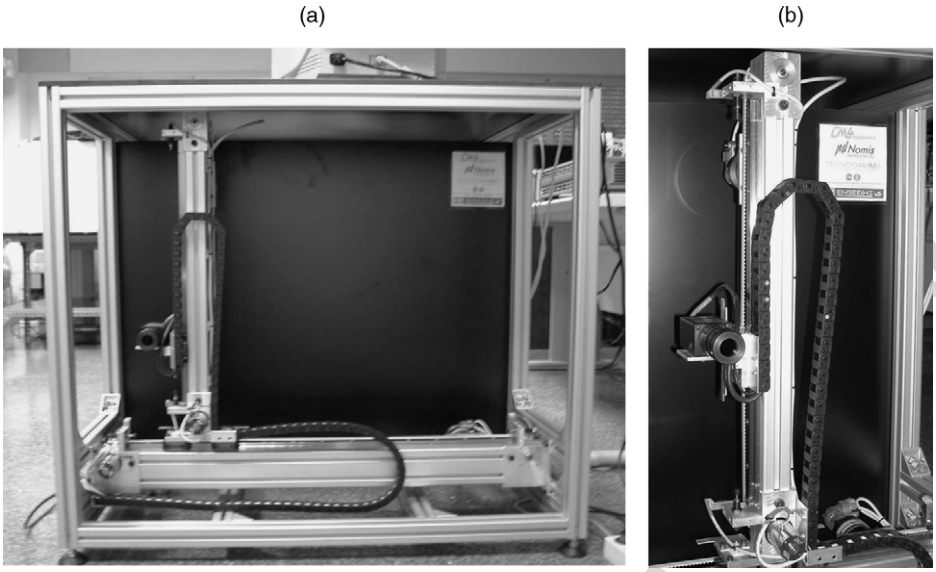

Fig. 2. (a) Mechanical set-up to displace the sensor along *X*- and *Y*-axis. (b) Detail of the sensor in the vertical axis.

visible wavelengths were always below 2% of its nominal value, with an average of 1% in all the neutral filters available.

In order to keep the unit as cost-effective as possible, an eight-bit CCD camera was selected. The dynamic range of the sensor was further optimized by using an external shutter which automatically adjusted the optimum exposure time. The exposure time could be adjusted to a time frame which varied from 0.099 to 16.419 ms, depending on the illumination of each of the registers at the measurement plane. The complete setup is controlled by a single PC, which controls the motors for sensor displacement, performs the automated data acquisition procedures, adjusts the scanning parameters, computes the final illumination distribution in the final plane and displays the obtained results.

CCD cameras have been routinely used as photometers for different applications, although several considerations are needed to ensure a correct photometric distribution measurement [7,8]. A linear output signal, a photopic spectral response, a uniform spatial response and negligible dark image signal are requirements of the system to be ensured for its proper functioning. All of them have been checked experimentally and, when required, the proper corrections have been included in the software [9].

Although the CCD sensor response is generally linear when related to the illumination value, in our case the presence of an external shutter for exposure control made it necessary to validate the linearity of the complete sensor. To evaluate the impact of the shutter on the sensor performance an LED with emission controlled through the circulating intensity was placed in front of the sensor, and several images for different exposure times and illuminations were recorded. The non-linearity factor, defined as ratio between maximum deviation and maximum signal value, was less than 0.8%.

Regarding the spectral response of the sensor, a combination of photopic and equalizing filter has been used to yield a spectral response as close as possible to the photopic response of the eye. The spectral response of the complete sensor (camera, lens, photopic and equalizing filter) has been measured using the light coming out of a monochromator assembled to a daylight vapour fluorescent lamp. The emitted energy was then measured both with a calibrated radiometer and with the sensor. Measurements have been performed in the 480–690 nm range in intervals of 10 nm. The ratio of grey levels and radiation yields the relative spectral response at each considered wavelength. Fig. 3 plots the measured spectral response of our sensor against the standard CIE photopic response.

The mismatch of a spectral response related to the photopic curve is usually measured using the f_1' parameter:

$$f_1' = 100 \frac{\int_0^\infty |s(\lambda) - v(\lambda)|\, d\lambda}{\int_0^\infty v(\lambda)\, d\lambda} \quad (2)$$

which evaluates the deviation of the measured spectral response of the sensor $s(\lambda)$ against the standard photopic response of the eye $v(\lambda)$ [10]. Photometers are classified using its f_1' value, with the maximum quality detectors presenting f_1' values below 3%, and good quality detectors with values between 3% and 8%. The measured value for our sensor is 4.6%, classifying it as a good quality detector.

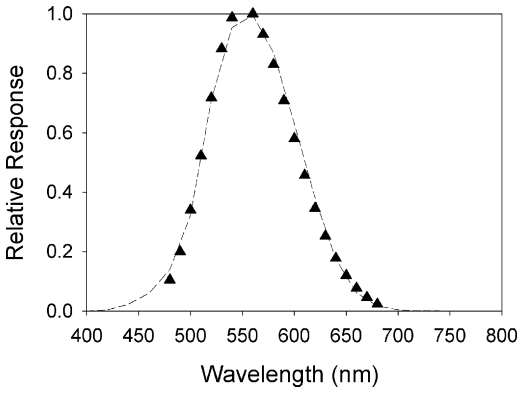

Fig. 3. Spectral calibration ((▲) sensor response–reference photopic response).

Author's personal copy

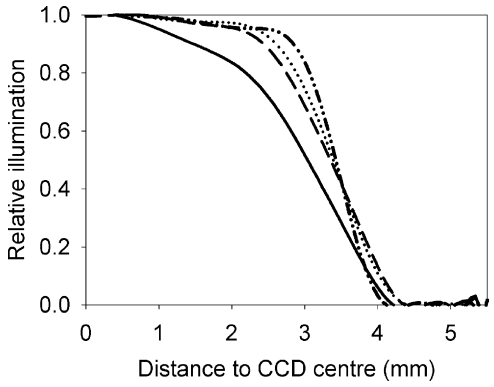

Fig. 4. Relative illumination along the CCD for different apertures: (—) $N = 1.7$, (– –) $N = 2$, (· · ·) $N = 2.8$, (– · · –) $N = 4$.

The remaining aspect to be taken into account is the non-uniformity response in the sensor, which could be a consequence of punctual defects or slight differences between pixel responses (surface, material, circuitry. . .). As these defects are completely random, a pixel by pixel correction factor would be required. Another type of non-uniformity response correction, linked to the optical performance of the sensor, is required to take into account the vignetting introduced by the optical system as well as by the $\cos^4 \theta$ law, which also locally change the energy measured at the sensor depending on the region of the CCD array.

Although in our sensor there are no detectable punctual defects, vignetting effects are clearly recognizable. The vignetting in the sensor involves a non-uniformity response of each pixel across the CCD sensor area due to the diameter and position of the lens and filter mounts. To measure the relative spatial response and introduce the proper correction factors, several registers have been recorded using a uniform illumination for different apertures ($N = 1.7$, 2, 2.8 and 4). Fig. 4 depicts the behavior of the sensor spatial response for each aperture, assuming radial symmetry for the lens and filter set. All curves may then be fitted to a simple polynomial function, so the relative energy loss at each pixel due to vignetting may be easily corrected.

Finally, several dark images have been recorded for different exposure times and the mean grey value for each exposure time has been determined and subtracted in each of the acquired registers.

4. Photometric calibration

Additional calibrations are needed in the unit in order to get real photometric distributions, and not merely relative grey level data, obtained in the final plane from the accumulation of the scaled and shifted registers obtained in the measurement plane. The photometric calibration of the unit pursues the conversion of accumulated grey level (GL) values in the final plane to illumination values (E) through a single constant K:

$$E = K(\mathrm{GL}) \tag{3}$$

The photometric constant has been obtained using two independent approaches. In a first approach, the linearity of the illumination–grey level relationship was confirmed using different illumination distributions measured at a plane 5 m away from the headlamp, yielding a K_E value. In a second approach, a step-by-step model of the different conversion factors which appear along the measurement chain was performed, yielding a K_T value. Then, each of these conversion factors was independently determined either through measurement or through calculation. Obviously, K_T and K_E should yield the same value.

Table 1
Working conditions for the photometric calibration experiments described in the text

Parameter	Value
Focal length (mm)	17.2 ± 0.05
Optical density of neutral filters (OD)	4.57 ± 0.01
Aperture Φ (mm)	10.1 ± 0.03
Displacement Δx (mm)	7.00 ± 0.01
Displacement Δy (mm)	7.00 ± 0.01
Distance of propagation $d_{M–F}$ (m)	5.00 ± 0.01

In the first approach, three photometric distributions with very different dynamics (driving beam, passing beam, fog lamp) were measured at a plane distant 5 m from the source, using both our unit and a calibrated radiometer. An array of 280 data points was obtained with the radiometer allowing a fair comparison with the continuous distribution obtained with our unit. Working conditions have been kept constant in all measurements and are summarized in Table 1.

Linearity has been verified through linear regression of illumination against accumulated grey level for each distribution taking both values at a given spatial position from the above-mentioned distributions. Fig. 5 depicts the relationship between illumination and accumulated grey value. The slope of each regression is the targeted calibration curve for the K_E value obtained experimentally. Table 2 presents the regression values and its experimental deviations.

Although the correlation coefficients are not as good as desired, mainly due to mismatches in the assignment of spatially equivalent points in both calibrations, deviation in K_E value keeps below 2%. As the working conditions have not changed, the mean calibration value may be measured with a deviation below 4%, yielding:

$$K_E = 1.16 \times 10^{-3}\ (\mathrm{lux/GL}) \tag{4}$$

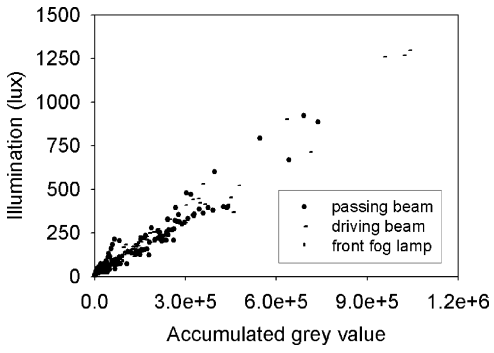

Fig. 5. Illumination vs. accumulated grey level for each distribution.

Author's personal copy

Table 2
Regression coefficients, deviations, and correlation coefficients for accumulated grey level value against illumination (lux)

	Regression coefficients ($y = ax + b$)	Coefficients deviations	r^2
Passing beam	$y = 1.116 \times 10^{-3}x + 7.099$	$\varepsilon_a = 0.012 \times 10^{-3}$; $\varepsilon_b = 2.858$	0.943
Driving beam	$y = 1.195 \times 10^{-3}x + 11.854$	$\varepsilon_a = 0.013 \times 10^{-3}$; $\varepsilon_b = 2.490$	0.976
Front fog lamp	$y = 1.178 \times 10^{-3}x + 3.775$	$\varepsilon_a = 0.012 \times 10^{-3}$; $\varepsilon_b = 0.587$	0.978

Such a value, however, is dependent in an unknown way on the experimental conditions of the measurement. In the second approach for photometric calibration, a theoretical calibration constant K_T will be determined from the multiplication of independent factors related to each of the key points of the measurement process. This not only allows the confirmation of the correct value for the previous constant, but enables in addition the measurement of the proper conversion factor whenever the working conditions of Table 1 are changed.

Such an approach requires proposing a model of the different factors affecting the grey level to energy conversion value. In our model, K_T will be divided into four more specific constants, related to the main four steps with relevant energy changes contained in the measurement chain: the optical density in the optics and filters (K_O), the ratio between the square sampled surface and the optics aperture (K_S), the relationship between grey level and illumination value at the sensor (K_{CCD}) and the distance from headlamp to the final plane (K_D). All of these constants are either known or easy to measure with simple experimental setups. Then:

$$K_T = K_O K_{CCD} K_S K_D \tag{5}$$

The first parameter (K_O) takes into account the energy lost due to the absorption of the optics elements (lens and filters), where D is the mean optical density of all these elements. This parameter has been experimentally measured yielding a value:

$$K_O = 10^D = 10^{D_{OPT}} 10^{D_{FLT}} = 3.72 \times 10^4 \quad \text{and} \quad D_{OPT} = 1.17\text{OD} \tag{6}$$

with D_{OPT} the optical density of the optics and photopic filters, and D_{FLT} the optical density of the neutral filters used in the particular setup considered. They have been considered separately as far as the neutral filters are the elements which are more likely to be changed when a different source is studied.

The conversion of the energy incident on the CCD camera into grey level values is related to the second factor K_{CCD}, which has been determined comparing the average grey level values of a given register with the incident illumination at the focal plane of the camera measured with a calibrated radiometer yielding a value of:

$$K_{CCD} = 4.46 \times 10^{-3}\ (\text{lux/GL}) \tag{7}$$

Obviously, another important factor to take into account is the scanning strategy of the instrument in the measurement plane (K_S), which is related to the sampled area on the measurement plane. This strategy may also vary depending on the requirements of the measurement. The energy incident in the sensor is limited by the diameter of the diaphragm (Φ), and, for a fixed diaphragm aperture, the accumulated grey level value is modified by the steps in the displacement of the sensor (Δx, Δy). The ratio of round area sampled by the lens aperture against the square area scanned from step to step on the plane depends only on known factors, and, for the working conditions in Table 1, yields:

$$K_S = \frac{\Delta x \Delta y}{\pi} \left(\frac{\Phi}{2} \right)^2 = 0.61 \tag{8}$$

Finally, the energy measured in the plane close to the headlamp will be projected onto the desired distant plane, where the illumination will vary according a factor depending on the focal length (f') of the lens and the distance between measurement plane and final plane (d_{M-F}). Again, in the working conditions of Table 1:

$$K_D = \frac{f'^2}{d_{M-F}^2} = 1.18 \times 10^{-5} \tag{9}$$

Using expression (5) we may see that all factors involved are already known, and that a K_T value can easily be calculated using the measured data in (6) and (7) and in expressions (8) and (9) together with the working conditions described in Table 1, yielding:

$$K_T = 1.19 \times 10^{-3}\ (\text{lux/GL}) \tag{10}$$

which is in very good agreement with the K_E value obtained in (4), confirming the general validity of the simple approach used. In consequence, the validity of the model used and of the factor decomposition along the measurement chain is proved. These findings are of great interest in case that some of the elements of the unit were changed, as only the factors affected by the recalibration of the unit would need to be recalculated.

5. Validation

Finally, the measurements of the calibrated unit have been validated by comparing three photometric distributions from a complex headlamp (passing beam, driving beam and front fog lamp) to the distributions measured in a photometric tunnel in a plane placed 25 m away from the headlamp, according to current headlamp testing normative. However, routine headlamp testing involves measuring a reduced number of positions (typically between 10 and 20 positions, depending on the type of headlamp or the type of lighting provided), which is a number too small to make reliable comparisons with the data obtained from the unit, which calculates thousands of points of the photometric distribution in the final plane. This has pushed to change the testing procedure in the photometric tunnel, which was modified in order to measure a square array of 51 × 31 data points so reli-

Author's personal copy

able comparison between both photometric distributions could be achieved. With our unit, we registered a square array of 800 registers with working conditions equivalent to those described in Table 1 but the propagation distance, which was changed to 25 m. It should be stressed that the point-by-point procedure in the photometric tunnel took over 45 min, while the measurement using the proposed measurement principle was obtained in less than 10 min, including the displacement of the sensor, data acquisition and calculation of the distribution at the desired final plane.

Fig. 6 compares both measurements for passing-beam, driving-beam and front fog lamp distributions of a complex headlamp in the central illumination area (6.64 m × 2.75 m). The contour plots show good comparison among each other with

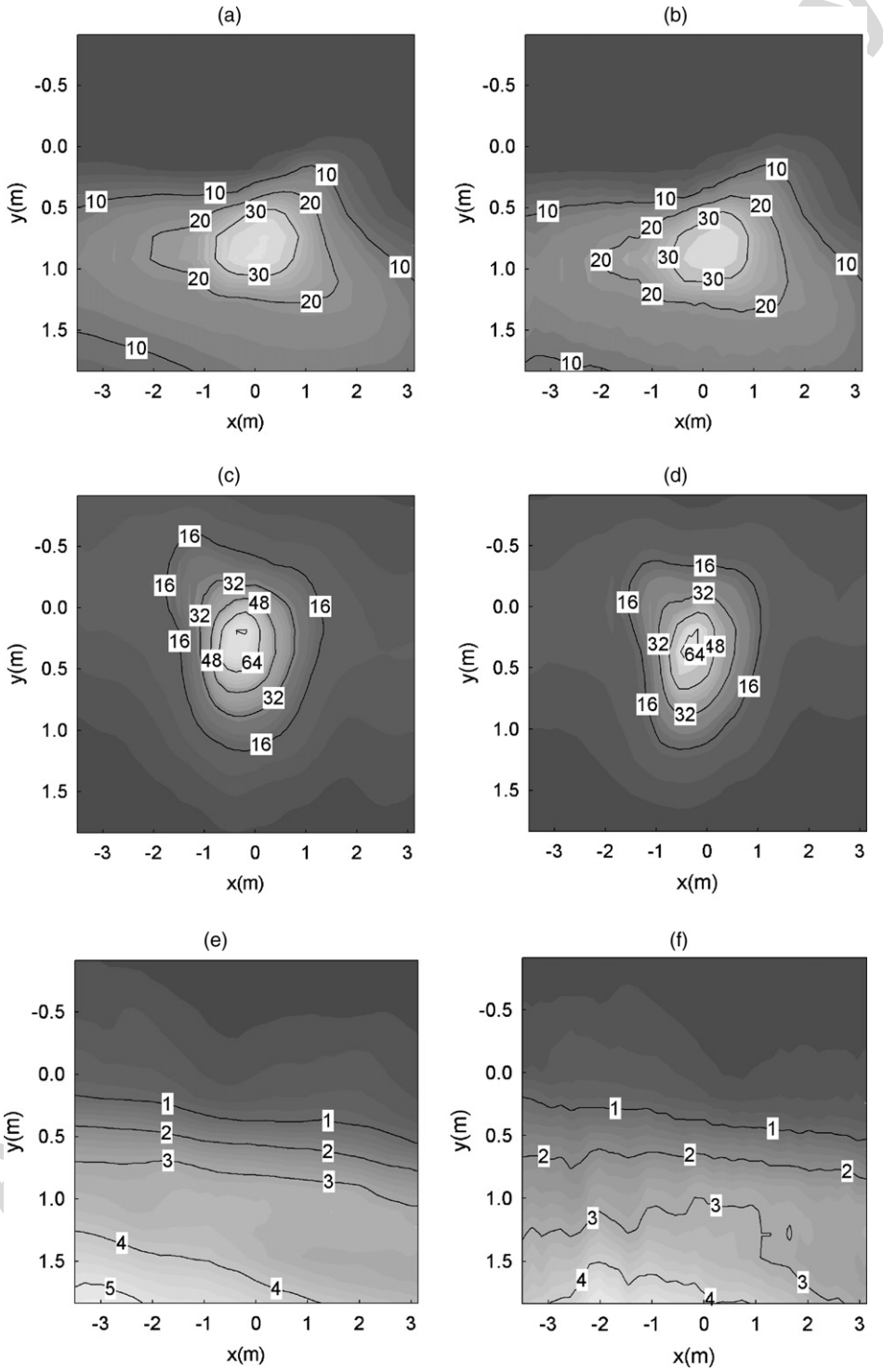

Fig. 6. Comparison of reference and measured photometric distributions from a complex headlamp. Passing beam (a) at the photometric tunnel; (b) with our unit. Driving beam (c) at the photometric tunnel; (d) with our unit. Front fog lamp (e) at the photometric tunnel (f) with our unit.

deviation of the measurements below 10% in the areas with higher energy. At lower energy areas (for instance, in front fog lamp distributions or the dark area of passing beam distributions) the effect of the small number of digitization bits appears in the shape of a larger measurement error, which becomes more evident because of the accumulation effect inherent to the measurement technique. This effect would be overcome using a higher number of digitization bits in the sensor.

6. Conclusion

A novel proposal for the characterization of photometric distributions in the far-field from measurements performed near the headlamp has been presented, avoiding the large space requirements or costly equipment nowadays in use for this purpose. The simple linear model proposed for setting a calibration value for the constant transforming accumulated grey levels at the final plane to photometric units has been proved to be valid, opening the possibility of changes in part of the unit without global recalibrations. Distributions measured using a prototype unit have been successfully compared with the measurements performed in photometric tunnels yielding equivalent results, especially in the areas with larger energetic values.

Although the results presented in this paper refer to automotive headlamps, the system has been successfully applied to the characterization of other extended sources, such as pilots, LEDs or luminaries. The system provides so much information on the source far-field photometric distribution that it could be used to calculate the distributions on any distant surface. In the case of headlamps, for instance, this can be easily applied to simulate the headlamp distribution on traffic relevant objects, such as traffic signs or roads. For the case of luminaries, the capabilities of the system could be applied to the simulation of the far-field pattern on roads or streets, and thus to the optimization of source positions in street lights or stadium lighting design, for instance. In our opinion, the system could be very useful in the countless applications where far-field pattern calculations from complex extended sources is required.

Acknowledgements

The authors wish to thank the European Union for its economic support in this research, funded through the GROWTH V Framework Program through the CRAFT project contract G3ST-CT-2002-50345. We also would like to thank Joan Fonts from IDIADA for his help and support.

References

[1] European Commission White Paper, European Transport Policy for 2010: Time to Decide, Office for Official Publications of European Communities, Luxembourg, 2001.
[2] National Highway Traffic Safety Administration Traffic Safety Facts 2000: A Compilation of Motor Vehicle Crash Data from the Fatality Analysis Reporting System and the General Estimates System, US Department of Transportation, Washington, 2001.
[3] J. Moisel, Solid state night vision system, Proc. SPIE 5663 (2004) 1–6.
[4] Economic Commission for Europe, Regulation N112: Motor Vehicle Headlamps Emitting an Asymmetrical Passing Beam or a Driving Beam or Both and Equipped with Filament lamps, 2001.
[5] Economic Commission for Europe, Regulation N113: Motor Vehicle Headlamps Emitting a Symmetrical Passing Beam or a Driving Beam or Both and Equipped with Filament Lamps, 2001.
[6] J. Arasa, S. Royo, J. Caum, M.J. Arranz, Measurement of the photometric distribution of light sources by deflectometric techniques, Proc. ETFA (2001) 695–698.
[7] I. Lewin, J. O'Farrell, Luminaries photometry using video camera techniques, J. Illum. Eng. Soc. 57 (1999) 63.
[8] M.S. Rea, I.G. Jeffrey, A new luminance and image analysis system for lighting and visions, J. Illum. Eng. Soc. 19 (1990) 64–72.
[9] M.J. Arranz, S. Royo, J. Arasa, M. Cattoen, NICOLAU: compact unit for photometric characterization of automotive lighting from near-field measurements, Proc. SPIE 5663 (2004) 76–85.
[10] De Cusatis, Handbook of Applied Photometry, American Institute of Physics, New York, 1992.

Biographies

Santiago Royo, completed his PhD in Applied Optics in 1999 in the Technical University of Catalunya, where he teaches on Optical Technology and Ophthalmic Lenses. He is also a senior researcher in the Center for Sensor, Instrumentation and Systems Development. His research interests involve optical metrology and fabrication topics, photometric testing and adaptive optics. E-mail: royo@oo.upc.edu.

María Jesús Arranz completed her BSc degree in Physics at the University of Barcelona in 1999. From 1999 to 2005 she was a teaching assistant at the Technical University of Catalunya. At present she is working as a researcher in Optical Engineering at the Center for Sensor, Instrumentation and Systems Development. Her work focuses on optical measurement techniques. She is currently pursuing her PhD degree. E-mail: mjesus@oo.upc.edu.

Josep Arasa got his BSc in Physics from University of Barcelona in 1980 and its PhD in Physical Sciences from University of Barcelona in 1988. He joined the School of Optics and Optometry of the Technical University of Catalunya in 1983 as an Assistant Lecturer, and lately became a Lecturer (1987), then a Professor (1992). From the beginning of his career, he has been involved in industrial applications of Optical Design and Optical Metrology. E-mail: arasa@oo.upc.edu.

Michel Cattoen got his PhD from Université Paul Sabatier in 1975 and his Doctorate of Sciences Degree from the National Polytechnic Institute of Toulouse (INPT) in 1985. He joined the Engineering School ENSEEIHT in 1974 as a Research Assistant, where he became first Lecturer (1986), and then Professor (1990). He is presently a Second Class Professor in the same institution. From the beginning of his career, he has been involved in Television and Image Processing, mainly in industrial applications (Computer Vision). His research themes concern applications in industrial vision and optoelectronics metrology. E-mail: michel.cattoen@len7.enseeiht.fr.

Thierry Bosch got his PhD from National Institute of Applied Science of Toulouse (INSAT) in 1992. He was a head of group on optoelectronics, instrumentation and sensors from 1993 to 2000. He is presently a second-class professor in the Engineering School ENSEEIHT of Toulouse and Director of Electronics Laboratory of ENSEEIHT (LEN7). His research interests are related to laser industrial instrumentation development including interferometry, phase-shift and self-mixing-based range finding techniques, vibration and velocity measurements E-mail: bosch@len7.enseeiht.fr.

Author's personal copy